

Preparation and Fluorescence Spectrum of Amorphous Huntite $\text{EuAl}_3(\text{BO}_3)_4$

SETSUHISA TANABE,* KAZUYUKI HIRAO,† NAOHIRO SOGA,†
AND TEICHI HANADA*

*Department of Chemistry, College of Liberal Arts & Sciences,
and †Department of Industrial Chemistry, Faculty of Engineering,
Kyoto University, Sakyo-ku, Kyoto 606-01, Japan*

Received August 30, 1991

A single crystal and an amorphous solid of $\text{EuAl}_3(\text{BO}_3)_4$ were prepared and their fluorescence properties were compared each other. It was found that the ${}^5D_0 \rightarrow {}^7F_0$ transition in the amorphous state, which is forbidden for Eu^{3+} ions at D_{3h} symmetry in the huntite crystal structure, was allowed and a decrease of the ligand field symmetry around the Eu^{3+} ion was suggested with the glass formation. The results of ${}^{151}\text{Eu}$ -Mössbauer effect and $\text{AlK}\alpha$ emission spectroscopy showed that the coordination number of Eu^{3+} ions increased from 9 to 12 and that of Al^{3+} ions almost decreased from 6 to 4 by glassification. The increase of the linewidth of both the fluorescence and Mössbauer spectra could be attributed to the site variation and ligand asymmetry of Eu^{3+} ions in the glass of this system. © 1992 Academic Press, Inc.

Self-concentration quenching reduces the efficiency of most rare-earth based luminescent materials because the non-radiative decay process occurs due to the electric-dipole coupling between rare-earth ions (I). Thus, in most glass systems doped with luminescent ions such as Nd-doped oxide glasses, the maximum content of Nd^{3+} ions is usually limited to much less than ~ 5 mol%. On the other hand, in some kinds of phosphate glasses, a large amount of rare-earth ions can be doped as a main component of glass composition without the concentration quenching, such as $\text{Eu}(\text{PO}_3)_3$ (I). The rare-earth aluminoborate crystal, $\text{LnAl}_3(\text{BO}_3)_4$ (2, 3) is a highly concentrated rare-earth crystal in stoichiometry along with $\text{Ln}_3\text{Al}_5\text{O}_{12}$ (4), $\text{Li}_6\text{Ln}(\text{BO}_3)_3$ (5, 6), and $\text{LnMgB}_5\text{O}_{10}$ (7). This crystal structure is isomorphous with huntite $\text{CaMg}_3(\text{CO}_3)_4$ (8).

Among the rare-earth huntite groups, $\text{NdAl}_3(\text{BO}_3)_4$ is known as a minilaser device (NAB) utilizing the fluorescence of the ${}^4F_{3/2} \rightarrow {}^4I_{11/2}$ transition of the Nd^{3+} ion (9). In addition to the benefit of unusual weak self-concentration quenching in these crystal groups, the possibility of glass formation in this system is of interest, because it contains a large amount of network-forming compounds such as B_2O_3 and Al_2O_3 . Thus it is attractive to investigate the fluorescence property of the glassy state, which is surely expected to accompany the structural change, under the same composition as that of crystal.

In this study, a single crystal of $\text{EuAl}_3(\text{BO}_3)_4$ huntite was prepared by the usual flux method and its fluorescence property was examined. In this structure, the ${}^5D_0 \rightarrow {}^7F_0$ transition of the Eu^{3+} ion is forbidden

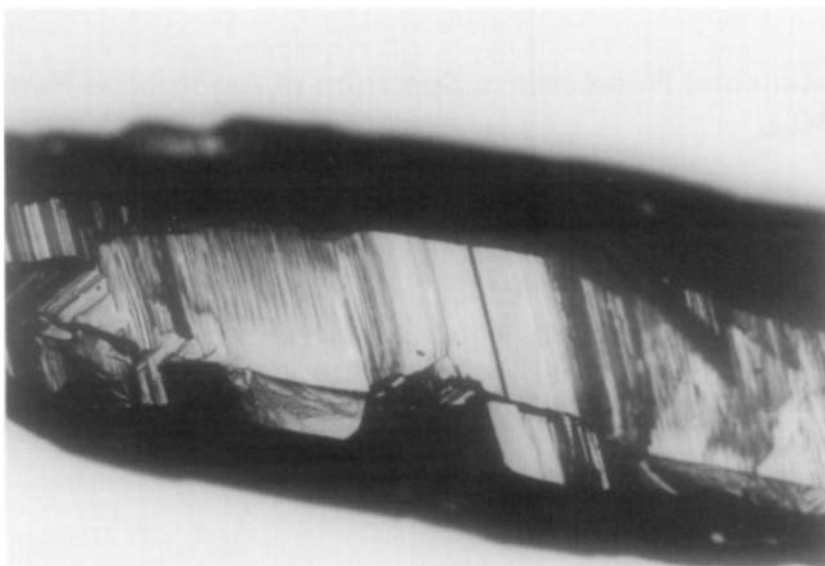


FIG. 1. $\text{EuAl}_3(\text{BO}_3)_4$ single crystal prepared by the flux method.

due to the site symmetry of $D_{3h}(4)$. In order to investigate the effect of glass formation on the structure and fluorescence property, an amorphous thin film was prepared by the twin-roller quenching method. The coordination numbers of Eu^{3+} and Al^{3+} ions were also investigated by the ^{151}Eu -Mössbauer and $\text{AlK}\alpha$ emission spectra, respectively.

A single crystal was obtained by using the $\text{Li}_2\text{O}-\text{B}_2\text{O}_3$ flux method, which was reported for $\text{NdAl}_3(\text{BO}_3)_4$ elsewhere (10). The composition shown in Table I was melted in a platinum crucible at 1200°C for 2 hr and the melt was slowly cooled at a rate of 10 K/hr down to 500°C . The solid obtained was etched with 0.1N HCl aqueous solution to avoid the lithium borate flux. The photograph of the obtained single crystal is shown in Fig. 1. The crystals obtained were a hexagonal rod in shape and pinkish in color with transparency. The X-ray diffraction analysis was carried out to confirm the formation of a pure phase in the powder form. No impurity phase was observed, and all the peaks could be assigned to the $\text{EuAl}_3(\text{BO}_3)_4$ huntite crystal.

The glassification of this crystal was conducted by using the twin-roller super cooling method. The rollers rotate themselves at a rate of about 1000 rpm. The glassy phase was confirmed by XRD. The DTA curve is shown in Fig. 2. The glass transition was clearly observed around 730°C as an endothermal step, and crystallization temperature, T_{cr} of the first exothermal peak was 830°C . This value of T_g is much higher than that of other alkali borate glasses, which is probably due to the absence of a network modifier such as alkali ions. Fluorescence

TABLE I
COMPOSITIONAL RATIO OF FLUX

Source	Ratio
Li_2CO_3	1
B_2O_3	3.22
Eu_2O_3	0.5
Al_2O_3	1.5

Note. Batch composition used for preparation of single crystal.

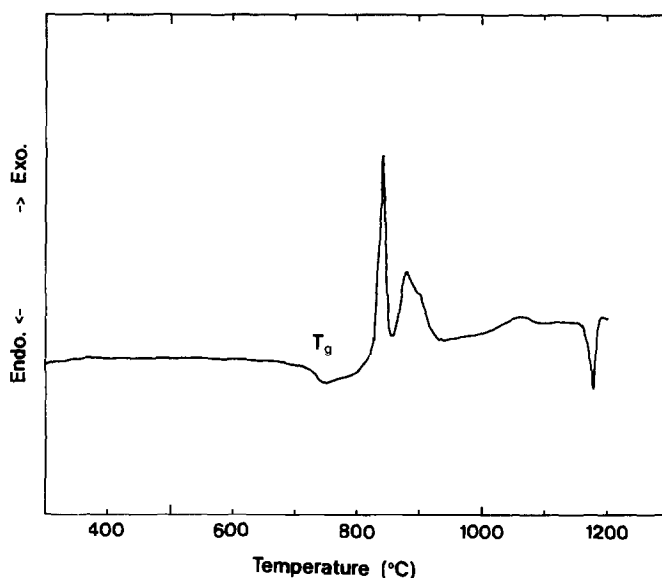


FIG. 2. DTA curve of amorphous sample.

spectra of the crystalline and amorphous sample were measured with a Hitachi-850 Fluorescence Spectrophotometer and are shown in Fig. 3. The excitation source was a Xe-lamp and the wavelength was 394 nm ($^5L_6 \rightarrow ^7F_0$). For the crystal sample, the spectrum was the same as that reported elsewhere (3). The $^5D_0 \rightarrow ^7F_0$ transition around 580 nm was not observed, since this transition is forbidden for Eu^{3+} ions at D_{3h} symmetry, as in $\text{EuAl}_3(\text{BO}_3)_4$ (3) and $\text{YAl}_3(\text{BO}_3)_4:\text{Eu}^{3+}$ huntite structures (11). On the other hand, this emission line was clearly observed for the glass sample. This phenomenon can be ascribed to the change in the site symmetry of each Eu^{3+} site from a crystalline to a glassy state. The splitting of 7F_1 and 7F_2 states became large due to the crystal field Stark splitting, but the fine structure could not be clearly observed because of site-to-site variation which is characteristic of the amorphous samples.

In Fig. 4, the ^{151}Eu -Mössbauer spectra of crystalline and glass samples are shown. The measurement was carried out by using

$^{151}\text{Sm}_2\text{O}_3$ (5 mCi) as a γ -ray source. The velocity calibration was done with the spectrum of $\alpha\text{-Fe}$ by the $^{57}\text{Co}(\text{Rh})$ source, and the isomer shift was determined with respect to that of EuF_3 . From Fig. 4, it can be seen that no Eu^{2+} ion (IS ~ -12 mm/sec) was formed, and the linewidth of the absorption peak due to Eu^{3+} ions became large for the glass sample. This line broadening can be due to the formation of site variation and to

TABLE II
THE CHEMICAL SHIFT OF $\text{AlK}\alpha$ EMISSION

Sample	Coordination number	Chemical shift (10^{-5} nm)
$\text{EuAl}_3(\text{BO}_3)_4$ crystal	6	27
amorphous	?	16
$\alpha\text{-Al}_2\text{O}_3$	6	20
$\nu\text{-Al}_2\text{O}_3^a$	5	17
Mullite	4.8	16
K-feldspar	4	11

^a Prepared by rf-sputtering.

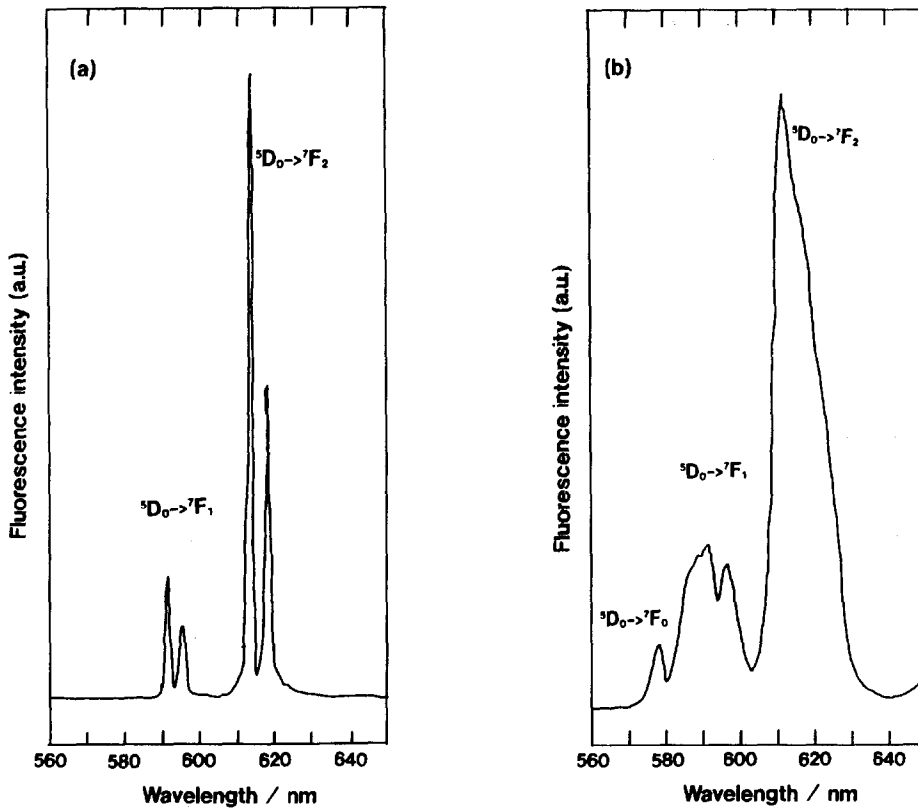


FIG. 3. Fluorescence spectra of (a) crystal and (b) amorphous sample.

the increase of the electric field gradient at ^{151}Eu nuclei in a random glass structure. The isomer shift, IS of Eu^{3+} ions in the glass sample was 0.30 mm/sec, while that of huntite crystal was 0.70 mm/sec. According to our previous study concerning about the relationship between IS and coordination numbers (CN = 6, 8, 9, 12) of Eu^{3+} ion in various oxide crystals (12), IS of Eu^{3+} ion can be a measure of the coordination number. For example, the IS of C- Eu_2O_3 (CN = 6) was 1.07 mm/sec and that of Eu- AlO_3 (CN = 12) was 0.52 mm/sec. Thus, it is suggested that the coordination number of Eu^{3+} ions in the glass sample increases up to 12.

In order to investigate the coordination

number of Al^{3+} ions accompanied with the structural change, the chemical shift of $\text{AlK}\alpha$ emission was determined with an X-ray probe microanalyzer. The results are shown in Table II together with the chemical shifts of $\alpha\text{-Al}_2\text{O}_3$, amorphous- Al_2O_3 , and mullite crystal. It can be seen that the chemical shift of the single crystal corresponds to that of the six-folded state, while that of the glass sample corresponds to that of the mullite crystal, where the average coordination number of Al^{3+} ions is 4.8. The change of the chemical shift in the same composition was -11×10^{-5} nm. This change in chemical shift is much larger than that for Al_2O_3 (-3×10^{-5} nm) in which the average coordination number of Al^{3+} changed from

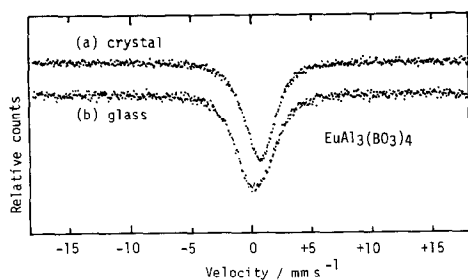


FIG. 4. The ^{151}Eu -Mössbauer spectra of (a) crystal and (b) amorphous sample.

6 to 5 with amorphous formation by rf-sputtering (13). Therefore, the coordination number of most Al^{3+} ions in the present system is considered to decrease from 6 to 4 by glassification. These four-folded Al^{3+} ions probably contribute to the network formation along with B^{3+} , while the Eu^{3+} ions work as the network modifier, taking higher-folded states.

In order to study the phonon mode cou-

pled with Eu^{3+} in these compounds, the phonon sideband associated with the $^5D_2 \leftarrow ^7F_0$ transition (14) was investigated. The excitation spectra of the crystal and glass are shown in Fig. 5(a) and (b), respectively. At higher energy side of the $^5D_2 \leftarrow ^7F_0$ electronic transition, the phonon sideband can be observed. The phonon energy which can be obtained as the energy difference between those peaks, was 1290 cm^{-1} for the crystal. This energy is exactly equal to that of the stretching vibration of BO_3^{3-} orthoborate group (15). This high energy phonon reduces the fluorescence lifetime by a rapid multiphonon decay process as in the $\text{NdAl}_3(\text{BO}_3)_4$ (3). By glassification, although the energy of phonon did not change drastically, the electron-phonon coupling strength, which is the intensity ratio of the phonon sideband to that of pure electronic transition, decreased drastically from 5×10^{-2} to 6×10^{-3} . In the glass, the chemical bonding with the highest phonon energy is

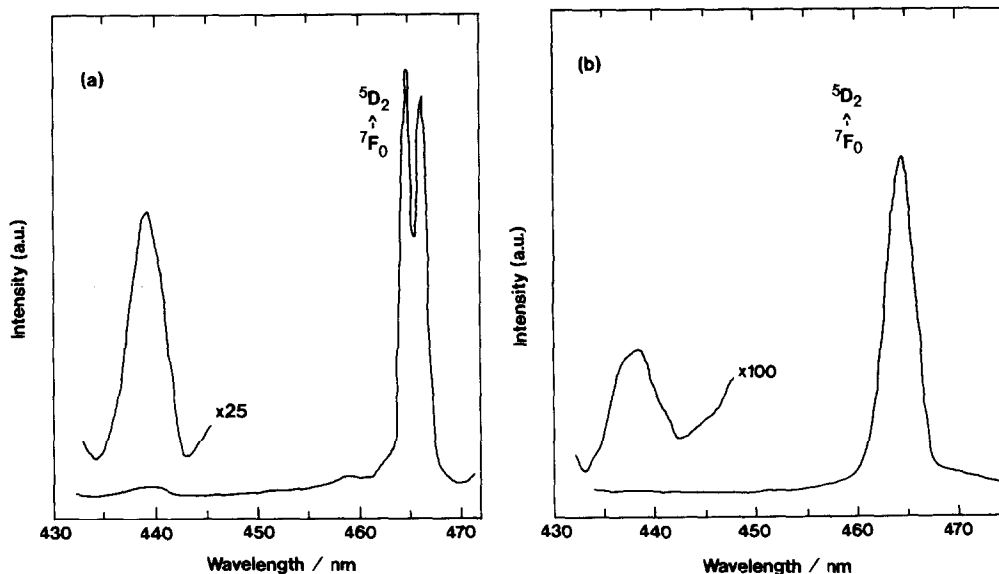


FIG. 5. Excitation spectra of $\text{Eu}^{3+} : ^5D_0 \rightarrow ^7F_2$ emission: (a) crystal and (b) amorphous sample. The phonon sideband associated with $^5D_2 \leftarrow ^7F_0$ electronic transition is observed at the higher energy side.

considered still to be ${}^3\text{B}-\text{O}$, although the CN change of some B atoms might occur from 3 to 4 accompanied with the CN change of Al^{3+} and Eu^{3+} . However, it is plausible that the network-modifying Eu^{3+} is placed near the nonbridging oxygen of ${}^3\text{B}-\text{O}^-$. Therefore, the phonon energy coupled with the multiphonon relaxation can be still about 1300 cm^{-1} of ${}^3\text{B}-\text{O}$ rather than ${}^4\text{B}-\text{O}$ with lower phonon energy ($\sim 1100\text{ cm}^{-1}$). As mentioned above, the electron-phonon coupling strength changed with structural change. This can be ascribed to two reasons. One is the decrease in the number of three-folded borons, which generates a decrease of the number of the ${}^3\text{B}-\text{O}$ bond. Another is the decrease of the mean free path of the phonon in amorphous structures. Further study is needed to clarify the structure of this amorphous as well as the electron-phonon coupling of rare earth ions.

In conclusion, the present work revealed the huntite crystal $\text{EuAl}_3(\text{BO}_3)_4$ can be vitrified by twin-roller quenching, accompanying the coordination change of Al^{3+} and Eu^{3+} ions. The fluorescence properties of Eu^{3+} drastically changed under the same composition, i.e., the forbidden ${}^5D_0 \rightarrow {}^7F_0$ transition at D_{3h} symmetry became allowed by the structural change. Also, the electron-phonon coupling strength decreased in the amorphous state.

Acknowledgments

The authors thank Dr. Y. Isozumi and Dr. S. Ito at the Radioisotope Research Center at Kyoto University for the ${}^{151}\text{Eu}$ -Mössbauer effect measurement.

References

1. M. J. WEBER, *Phys. Rev. B* **4**(9), 2932 (1971).
2. H. Y-P. HONG AND K. DWIGHT, *Mater. Res. Bull.* **9**(12), 1661 (1974).
3. F. KELLENDONK AND G. BLASSE, *J. Chem. Phys.* **75**(2), 561 (1981).
4. J. P. VAN DER ZIEL, L. KOPFF, AND L. G. VAN UITERT, *Phys. Rev. B* **6**(2), 615 (1972).
5. F. W. TIAN, C. FOUASSIER, AND P. HAGENMULLER, *J. Phys. Chem. Solids* **48**(3), 245 (1987).
6. J. MASCETTI, C. FOUASSIER, AND P. HAGENMULLER, *J. Solid State Chem.* **50**, 204 (1983).
7. C. FOUASSIER, B. SAUBAT, AND P. HAGENMULLER, *J. Lumin.* **23**, 405 (1981).
8. D. L. GRAF AND W. F. BRADLEY, *Acta Crystallogr.* **15**, 238 (1962).
9. G. HUBER, in "Current Topics in Material Science" (E. Kaldis, Ed.), Vol. 4, pp. 1-45, North-Holland, Amsterdam (1980).
10. S. OHISHI, C. NISHIKAWA, AND I. TATE, *Chem. Express* **2**(10), 647 (1987).
11. W. C. NIEUWPOORT, G. BLASSE, AND A. BRIL, in "Optical Properties of Ions in Crystals", (H. M. Crosswhite and H. W. Moos, Eds.), pp. 161-168, Interscience, New York (1967).
12. S. TANABE, K. HIRAO, AND N. SOGA, *J. Non-Cryst. Solids* **113**, 178 (1989).
13. T. HANADA AND N. SOGA, *J. Am. Ceram. Soc.* **70**(12), C-362 (1987).
14. S. TANABE, S. TODOROKI, K. HIRAO, AND N. SOGA, *J. Non-Cryst. Solids* **122**, 59 (1990).
15. W. L. KONIJNENDIJK AND J. M. STEVELS, *J. Non-Cryst. Solids* **18**, 307 (1975).